Journal of Steroid Biochemistry and Molecular Biology xxx (xxxx) xxx–xxx

Contents lists available at ScienceDirect

Journal of Steroid Biochemistry and Molecular Biology

journal homepage: www.elsevier.com/locate/jsbmb

Full length article

Antitumoral effects of the alkynylphosphonate analogue of calcitriol EM1 on glioblastoma multiforme cells

María Julia Ferronato[a,1], Eliana Noelia Alonso[a,1], Débora Gisele Salomón[a], María Eugenia Fermento[a], Norberto Ariel Gandini[a], Mario Alfredo Quevedo[b], Evangelina Mascaró[c], Cristian Vitale[c], Yagamare Fall[d], María Marta Facchinetti[a], Alejandro Carlos Curino[a,*]

[a] Laboratorio de Biología del Cáncer, Instituto de Investigaciones Bioquímicas de Bahía Blanca (INIBIBB), Universidad Nacional del Sur (UNS), CONICET, Departamento de Biología, Bioquímica y Farmacia (UNS), Bahía Blanca, Argentina
[b] Unidad de Investigación y Desarrollo en Tecnología Farmacéutica (UNITEFA-CONICET), Facultad de Ciencias Químicas, Ciudad Universitaria, Universidad Nacional de Córdoba, Córdoba, Argentina
[c] Laboratorio de Química Orgánica, Instituto de Química del Sur (INQUISUR), Universidad Nacional del Sur (UNS), CONICET, Departamento de Química (UNS), Bahía Blanca, Argentina
[d] Departamento de Química Orgánica, Facultad de Química e Instituto de Investigación Biomédica (IBI), Universidad de Vigo, Campus Lagoas de Marcosende, 36310 Vigo, Spain

ARTICLE INFO

Keywords:
Glioblastoma multiforme
Analogue
Vitamin D
Calcitriol
EM1
Antitumoral

ABSTRACT

Glioblastoma multiforme (GBM) is the worst and most common brain tumor, characterized by high proliferation and invasion rates. The current standard treatment is mainly based on chemoradiotherapy and this approach has slightly improved patient survival. Thus, novel strategies aimed at prolonging the survival and ensuring a better quality of life are necessary. In the present work, we investigated the antitumoral effect of the novel analogue of calcitriol EM1 on GBM cells employing in vitro, in silico, and in vivo assays. In vitro, we demonstrated that EM1 treatment selectively decreases the viability of murine and human tumor cells without affecting that of normal human astrocytes. The analysis of the mechanisms showed that EM1 produces cell cycle arrest in the T98G cell line, which is accompanied by an increase in p21, p27, p57 protein levels and a decrease in cyclin D1, *p*-Akt-S473, *p*-ERK1/2 and c-Jun expression. Moreover, EM1 treatment also exerts in GBM cells anti-migratory effects and decreases their invasive capacity by a reduction in MMP-9 proteolytic activity. In silico, we demonstrated that EM1 is able to bind to the vitamin D receptor with greater affinity than calcitriol. Finally, we showed that EM1 treatment of nude mice administered at 50 ug/kg body weight during 21 days neither induces hypercalcemia nor toxicity effects. In conclusion, all the results indicate the potential of EM1 analogue as a promising therapeutic alternative for GBM treatment.

1. Introduction

Glioma is the most prevalent malignant carcinoma of the central nervous system [1]. According to the WHO (World Health Organization) classification, based on the degree of malignancy, gliomas are divided into grade I/II (low grade) and grade III/IV (high grade) [2]. Glioblastoma multiforme (GBM), a WHO-defined grade IV astrocytoma, is the most common and aggressive form of primary brain tumor and encompasses 65% of all gliomas [2,3]. GBM is characterized by high proliferative rate, necrosis, high vascularization and infiltrating growth, and is associated with high rates of recurrence, overall resistance to therapy, devastating neurological deterioration, and low survival rates [4]. All of them make GBM one of the most lethal forms of cancer. Despite advances in the understanding of its pathophysiology, GBM remains incurable with therapy options that contribute little to prolong the survival time. Currently, under standard treatment regimen, which includes resection plus adjuvant chemoradiotherapy, GBM patients have a median survival of 12–15 months and less than 5% survive longer than 5 years [2,4,5]. Thus, there is a clear need to develop new therapeutic agents targeting GBM.

* Corresponding author at: Laboratorio de Biología del Cáncer, Instituto de Investigaciones Bioquímicas de Bahía Blanca (INIBIBB-UNS-CONICET), Centro Científico Tecnológico Bahía Blanca, Camino La Carrindanga Km. 7 – C.C. 857, 8000, Bahía Blanca, Argentina.
E-mail addresses: acurino@criba.edu.ar, juliaferronato@gmail.com (A.C. Curino).
[1] These authors contributed equally to this work.

http://dx.doi.org/10.1016/j.jsbmb.2017.10.019
Received 9 August 2017; Received in revised form 22 September 2017; Accepted 25 October 2017
0960-0760/ © 2017 Elsevier Ltd. All rights reserved.

1α,25-dihydroxyvitamin D_3 (calcitriol), the hormonally active form of vitamin D, is widely known for its role in the physiological regulation of calcium and phosphorous and in bone mineralization [6]. In addition to these classic activities, a large number of studies suggest that calcitriol play a protective role in the onset, progression and prognosis of several diseases, including cancer [7]. In this context, calcitriol has been shown to affect most of the "hallmarks of cancer" [8], among them: cell proliferation and differentiation, apoptosis, angiogenesis, cell invasion and metastasis, DNA repair, metabolism and inflammation [6,7,9]. It was demonstrated that calcitriol exerts these antitumoral effects through genomic and/or non-genomic pathways [6,10,11]. In both mechanisms of action the participation of the vitamin D receptor (VDR) has been described. Activation of VDR is highly dependent on the ability of ligands to produce an allosteric control on the Ligand Binding Domain (LBD) by eliciting a conformational modulation of the H12 helix. This induces a conformational change of the ligand-dependent transcriptional activation region AF-2, that allows the recruitment of co-modulators necessary to modulate the transcription process [12]. Furthermore, it was found that calcitriol shows highly tissue-specific effects [13] because the relative expression levels of these co-modulators is cell-specific determining that calcitriol exerts distinct functions in different cellular types [7].

With regard to gliomas, the potential antitumoral effect of calcitriol began to be considered after detecting the presence of VDR in human glial tumors [14]. It was demonstrated that calcitriol sensitivity varies between different glioma cell cultures. While in many cases calcitriol inhibits growth and induces apoptosis in several glioma cell lines and primary cultures [15–23], in other cases high resistance to calcitriol treatment is observed [19–21,24]. In light of this heterogeneous effect, we aimed at studying the expression of VDR in human gliomas to try to correlate the potential benefit of vitamin D compounds with the presence of this receptor. Indeed, we observed that VDR expression is associated with longer overall survival time in patients with GBM [25], supporting the antitumoral role of the vitamin D pathway in this particular type of glioma.

Based on data from preclinical studies, the anticancer activity of calcitriol requires supraphysiological doses and systemic exposure and before or simultaneous with cytotoxic drug administration. An early phase II trial of oral calcitriol in hormone refractory prostate cancer showed that 20–30% of patients receiving calcitriol in a daily basis developed hypercalcemia [26]. These studies prompted the search of ways to avoiding hypercalcemia. One of them was the election of intermittent doses of calcitriol or/and the combination with other compounds (i.e. dexamethasone) in clinical trials. However, the current available formulations of calcitriol are not ideal for antitumor treatment since it is difficult to achieve systemic stable levels of the drug [27]. Another way was the development of vitamin D analogues in the hope of alleviating hypercalcemia and increasing the anticancer properties of calcitriol [27]. In addition, taking into account that the catabolic enzyme 24 hydroxylase is aberrantly expressed in numerous human tumor types, including gliomas, elevated expression of this enzyme may stimulate calcitriol degradation and thus abrogate its antitumoral effects [28]. One way to overcome this problem is to employ calcitriol analogues that maintain the potent antitumoral effects, display less calcemic activity and elicit resistance to cellular catabolism initiated by C-24 hydroxylation. In this context, we had previously reported the design and synthesis of a novel phosphonate analogue of calcitriol called EM1 (Diethyl [(5*Z*,7*E*)-(1*S*,3*R*)-1,3-dihydroxy-9,10-6 secochola-5,7,10(19)-trien-23-in-24-yl] phosphonate analogue) [29]. The structural characteristics of this analogue combine the low calcemic potential of phosphonates [30] and the reduced metabolic inactivation given by the presence of a triple bond at C-24 [31]. In addition, we demonstrated that EM1 has anti-proliferative activity against a broad panel of murine and human tumor cell lines and lacks hypercalcemic activity in mice at 5 and 20 μg/kg body weight during a period of 5 days [29]. Furthermore, recently we reported that EM1 treatment decreases lung metastases in a murine model of hormone-independent breast cancer through its action on cell migration and invasion, without causing hypercalcemic effects [32]. However, its antitumoral potential in GBM is little known.

Therefore, the purpose of the current study is to investigate if EM1 is able to attenuate the aggressive phenotype of GBM. In addition, by applying state of the art molecular modeling techniques, we aim to investigate the intermolecular interaction between EM1 and VDR and the corresponding structural effects on AF-2. These studies will give information regarding the potential therapeutic use of EM1 in GBM.

2. Materials and methods

2.1. Chemicals and reagents

Diethyl [(5*Z*,7*E*)-(1*S*,3*R*)-1,3-dihydroxy-9,10-secochola-5,7,10(19)-trien-23-in-24-yl] phosphonate analogue (EM1) was reconstituted in 100% HPLC-grade isopropanol and stored protected from light at −20 °C. The design and synthesis of this alkynylphosphonate analogue of calcitriol EM1 were previously reported [29]. The amount of EM1 was determined by UV spectrophotometry between 200 and 300 nm. Drug was dissolved in isopropanol (vehicle) to the concentration of 10^{-3} M and subsequently diluted in the culture medium or in physiologic solution to reach the required concentration or doses employed for in vitro or in vivo assays. The maximal concentration of vehicle used in this study had no effect on cell viability, migration, adhesion and invasion.

2.2. Cell culture

Human U251 and T98G GBM cell lines were cultured in Dulbecco's Modified Eagle's Medium (DMEM, Sigma) supplemented with 10% (v/v) fetal bovine serum (FBS, Gibco), L-glutamine (5 mM, Gibco), penicillin (100 U/mL, Gibco), and streptomycin (100 mg/mL, Gibco,) at 37 °C in a humidified 5% CO_2 air atmosphere. Also, we employed the murine GL26 GBM cell line in viability assays that were maintained in Roswell Park Memorial Institute medium (RPMI, Sigma) supplemented with 10% FBS, L-glutamine, penicillin and streptomycin.

Human primary astrocytes were obtained from ScienCell Research Laboratories that provided cells isolated from human brain (cerebral cortex) and cryopreserved at passage one.

Alternately, T98G stably expressing a shRNA against vitamin D receptor (T98G-shVDR) or control shRNA (T98G-shCTRL) were used. Cells were transfected with pFIV-H1-Puro shRNA VDR or CTRL pFIV-H1-Puro vector plasmids using Lipofectamine 2000 (Invitrogen). Transfected cells were selected with 1 μg/mL puromycin (Merck) and the silencing of VDR was checked by western blot.

2.3. Cell viability assays

Murine GL26 and human U251 GBM cells were plated at a density of 800 cells/well and primary astrocytes at 3500 cells/well into 96 multiwell dishes in complete medium. Cells were treated with 0.01 to 100 nM of EM1, calcitriol or vehicle for 120 h, replacing the medium every 2 days. Then, they were washed with phosphate-buffered saline (PBS), trypsinized, suspended in 100 μL of complete medium, and counted manually using a hemocytometer. Additionally, cell viability was assessed by WST-1 colorimetric assay (Roche). For this purpose, following treatments, the cells were incubated for 1 h at 37 °C with the tetrazolium salt (4-[3-(4-Iodophenyl)-2-(4-nitrophenyl)-2H-5-tetrazolio]-1,3 benzene disulfonate) and the absorbance of the formazan product was read at 440 nm. The reference wavelength was 690 nm. The experiments were repeated twice and performed in quadruplicate.

2.4. Cell cycle analysis

Human T98G cells treated with EM1 (100 nM) or vehicle during 96 h were trypsinized, washed twice with ice-cold PBS, fixed with ice-cold 70% ethanol and incubated at −20 °C during 24 h. Then, the cells were stained with 50 μg/mL Propidium Iodide (PI, Roche) plus RNase A (100 μg/mL) in PBS and analyzed for DNA content by FACScan flow cytometry (Becton Dickinson). Data were analyzed using Cell Quest software (Becton Dickinson, Heidelberg, Germany). At least 100,000 cells were analyzed for each sample.

2.5. Cell migration assay

Cell migration was studied by employing the wound healing assay. Human T98G, T98G-shVDR, T98G-shCTRL and U251 cells were seeded in 35 mm Petri dishes and cultured until confluence. The cells were scraped with a 200 μL pipette tip denuding a strip of the monolayer, and fresh medium containing EM1 (100 nM) or vehicle was added to each plate. The photos were taken immediately after scraping (0 h) as well as 17 h later. Images were captured with an inverted microscope NIKON ECLIPSE TE 2000S, equipped with a digital camera (Nikon Coolpix S4, 6.0 Mpix, 10× zoom). The uncovered wound area was measured and quantified using Image J Analysis software.

2.6. Cell adhesion assay

Cell adhesion was evaluated as previously described [33]. Briefly, human T98G and U251 cells were pre-treated with vehicle, EM1 (100 nM) or calcitriol for 17 h. Then, cells were seeded into 96 multi-well dishes (10,000 cells/well, 4 wells for each condition) and were allowed to adhere. After 30 min non-adherent cells were removed by gentle washing with PBS. Attached cells were fixed in 100% methanol for 10 min and stained with 0.1% (w/v) crystal violet (Sigma) for 20 min. Cells attached to the culture plate were observed with an inverted microscope NIKON ECLIPSE TE 2000S, equipped with a digital camera (Nikon Coolpix S4, 6.0 Mpix, 10× zoom). For each replicate, ten randomly selected fields were photographed and the cells were counted with Image J Analysis software.

2.7. Cell invasion assay

The invasion of human T98G and U251 cells was assessed in transwell chambers (12 μm pore size, Millipore) with Matrigel (BD Biosciences) as previously described [33]. Briefly, each transwell was coated with 100 μL of a 1:3 Matrigel in cold serum-free DMEM to form a thin continuous film on top of the filter. The lower chamber was filled with 600 μL of DMEM containing 10% FBS. T98G or U251 cells (12,500 cells/well) in 500 μL of DMEM medium with vehicle, EM1 (100 nM) or calcitriol (100 nM) were transferred to each transwell in triplicate. After incubation for 17 h at 37 °C, the cells on the upper side of the transwell membrane were removed by cotton swab and rinsed with PBS. Invasive cells attached to the lower side of the membrane were fixed in 100% methanol for 10 min at room temperature and stained with 0.5% (w/v) crystal violet (Sigma) for 5 min. For each replicate, 10 randomly selected fields were photographed and the cells were counted with Image J Analysis software.

2.8. Gelatin zymography assay

Human T98G and U251 cells were plated at a density of 8000 cells/well into 96 multi-well dishes and grown to 80% confluence. The cells were treated with vehicle, EM1 (100 nM) or calcitriol in serum-free medium for 17 h. Conditioned media (CM) were individually collected, cold-centrifuged and stored at −20 °C. Then, they were run on 10% SDS-polyacrylamide gels containing 3 mg/mL of gelatin under non-reducing conditions. After electrophoresis, gels were washed for 20 min using 2.5% Triton X-100 and subsequently incubated for 24 h at 37 °C in agitation with buffer containing 50 mM Tris-HCl, 200 mM NaCl, 5 mM $CaCl_2$, and 0.02% Triton X-100 (pH 7.4). After incubation, gels were fixed and stained with 0.1% Coomassie Brilliant Blue G-250 in methanol/acetic acid/H_2O (30:10:60). Activity bands were visualized by negative staining. Gelatinolytic bands were visualized using a transilluminator and measured with Image J. Data were normalized to the amount of cells/well, determined by manual counting with a hemocytometer.

2.9. Western blotting

Human T98G and U251 cells were plated into dishes containing complete medium and treated with EM1 (100 nM) or vehicle for 30 min, 60 min or 48 h. The treatment time varies according to the protein under study and, particularly for evaluating the expression of phospho-Akt-S473 (pAkt-S473), phospho-ERK1/2 (pERK1/2) and c-Jun, cells were previously deprived of FBS for 18 h. Briefly, cell lysates were prepared by incubating the cell cultures in lysis buffer with protease inhibitors (Calbiochem) on ice for 30 min. Total protein concentrations were determined by Bradford assay using a Jasco V-630 spectrophotometer. Briefly, 50–85 μg of protein lysates were separated by SDS-PAGE on 12% and 15% gels and transferred onto nitrocellulose membrane. They were blocked with 5% non-fat dry milk for 30 min, incubated with a primary antibody, washed and then incubated with horseradish peroxidase-conjugated secondary antibodies. The reactions were detected by enhanced chemiluminescence (ECL) following the manufacturer's directions (Amersham, ECL Plus Western Blotting Detection Reagents, GE Healthcare). Primary antibodies used were mouse monoclonal anti-p21 (BD Biosciences, #556430), mouse monoclonal anti-p27 (BD Biosciences, #610241), mouse monoclonal anti-p57 (BD Biosciences, #556346), rabbit polyclonal anti-p53 (FL-393, Santa Cruz Biotechnology, sc-6243), rabbit monoclonal anti-Cyclin D1 (Thermo Scientific, #RM-9104-S), rabbit polyclonal anti-VDR (C-20) (Santa Cruz Biotechnology, sc-1008), rabbit polyclonal anti-*p*-Akt-S473 (Cell Signaling, #9271S), rabbit polyclonal anti-pERK1/2 (Cell Signaling, #9101), rabbit monoclonal anti-c-Jun (60A8) (Cell Signaling, #9165). Goat polyclonal anti-β-actin (C-11) (Santa Cruz Biotechnology, sc-1615) was used as internal control for protein loading and analysis. Data shown are representative of at least twice independent experiments.

2.10. Immunofluorescence (IF)

Human T98G cells were seeded on glass coverslips in 35 mm Petri dishes and cultured until 50% confluence. They were treated with EM1 (100 nM) or vehicle for 48 h. After treatment, they were washed three times with PBS and fixed with paraformaldehyde 4% in PBS. The cells were then permeabilized with 0.2% Triton in PBS and blocked with 1% bovine serum albumin (BSA) in PBS. After that, they were incubated with purified mouse monoclonal anti-p27 (BD Biosciences, #610241) in 1% BSA in PBS for 1 h. Then, the cells were washed with PBS and incubated with biotinylated goat anti-mouse IgG antibody (Vector Laboratories) for 1 h in dark. After that they were washed twice with PBS and finally cell nucleus were stained with 4′,6-diamidino-2-phenylindole (DAPI; 1:10,000 in PBS). The cells with nuclear p27 expression were counted in 10 randomly chosen fields of each condition.

2.11. RNA extraction and real-time qPCR

Total RNA was isolated from human T98G treated cells using TRIzol reagent (Life Technologies) and purified using SV total RNA isolation system (Promega). cDNAs were synthesized with MMLV- RT (Promega) and used for real-time PCR amplification with Taq PCR Master Mix 2× (Qiagen). Forward and reverse primers for the reaction were as follows: 5- CTGGAGACTCTCAGGGTCGAA-3′ (forward) and 5′-GGATTA

GGGCTTCCTCTTGGA-3′ (reverse) for p21; 5-TCGGCATGATGAA GGAGTTC-3 (forward) and 5-AGTCGGAGTAGGTGGGGTCGTAGG-3 (reverse) for VDR; 5′-GCTTTACCCAAAGGAATTGTCCGC-3′ (forward) and 5′-TCCCAGCACTCAGTCCGCTT-3′ (reverse) for CYP24A1; 5′-TTCACCACCATGGAGAAGGC-3′ (forward) and 5′-AGTGATGGCA TGGACTGTGGTC-3′ (reverse) for GAPDH. Each PCR was done in duplicate and the experiment was repeated twice. Data were analyzed using the $2^{-\Delta\Delta CT}$ method [34].

2.12. Evaluation of calcemic activity in mice

Animal study was conducted in accordance with the National Institutes of Health (NIH) Guide for the Care and Use of Laboratory Animals. The protocols were approved by the local ethic committee. Ten-week-old male N:NHI(S)-*Fox1*^{nu} mice, weighing around 25 g, were purchased from the Facultad de Ciencias Veterinarias (La Plata, Argentina). Mice were housed under pathogen-free conditions, in plastic cages, under controlled temperature and humidity, with a 12:12 h light-dark cycle and free access to food and water. Animals were acclimatized for at least one week before starting the experiment. Mice were randomly divided into two groups and were intraperitoneally injected with EM1 (n = 5) or vehicle (n = 4) at 50 μg/kg, three times a week (Monday, Wednesday and Friday) during three weeks (total doses = 9). Blood samples were collected at the beginning and at the end of the period treatment. To this end, mice were anesthetized as previously described [29] and blood from the retro-orbital sinus was obtained employing capillary tubes. Samples were held on ice, processed at 4 °C, and plasma was separated and stored at −20 °C until assayed. Approximately 40 μL of plasma/mouse was obtained. Calcium concentration was determined using Ca-Color Arsenazo III AA kit (Wiener Lab, Argentina), measuring the absorbance at 650 nm. The sample calcium concentration was calculated based upon calcium standards provided by the manufacturer. Additionally, the hematocrit for each mouse was analyzed before and following treatments to determine if the mice were healthy. Toxicity parameters were assessed by clinical measures, such as weight loss, changes in appearance and behavior, lethargy and death. Animal weight was evaluated during treatment period.

2.13. Liver and kidney histological analysis

Liver and kidney from EM1-treated mice and vehicle-treated mice were excised, quickly fixed in 10% formalin in PBS for 24 h, and processed into paraffin by standard procedures. Paraffin sections of 5 μm thick were obtained using a rotary microtome (Leica, RM 2155). Then, they were dewaxed, rehydrated in a decreasing series of ethanol dilutions and stained with Hematoxylin and Eosin (H & E). The histological examination was assessed by an expert pathologist. Ten randomly fields for each slide were analyzed.

2.14. Molecular modeling studies

The intermolecular interaction between EM1 and VDR was studied by applying molecular docking, molecular dynamics and free-energy of binding analyses. The structure corresponding to VDR (PDB code: 1DB1) was used as template [35], since it has been adequately validated as target structure [36]. The initial structure of EM1 was drawn using the MarvinSketch software [37], which was afterwards refined to obtain the minimum energy conformation using semiempirical (AM1) and ab initio (HF/6-311 + G*) methods as implemented in the Gaussian03 software [38].

Docking studies were performed in a multistep procedure using software packages developed by OpenEye Scientific Software [39]. In a first stage, libraries of conformers were generated for the ligand considering an energy threshold of 10 Kcal/mol and using the OMEGA software [40,41]. Next, conformers were subjected to docking studies by applying a fast rigid exhaustive docking approach implemented in the FRED3 software [42–44]. Finally, docked position were scored and ranked using the ChemGauss3 scoring function, with the lowest energy docked posed being identified for further analysis. Structural analyses and three dimensional visualization were performed by means of the VIDA [45] and LigPlot [46] software.

The lowest energy complex obtained by molecular docking was further analyzed by means of molecular dynamics simulations. In this case the AMBER16 software package was used to obtain and analyze the corresponding trajectories [47,48]. Atomic charges and molecular parameters for the ligand were assigned from restrained electrostatic potential fitted (RESP) fitted charges and the GAFF2 forcefied, respectively [49]. The charges and molecular parameters corresponding to VDR were assigned from the ff14SB forcefield [50]. Simulations were performed under explicit solvent conditions, using pre-equilibrated TIP3P explicit water molecules included in a cubic box. Solvated systems were subjected to the following simulation protocol: a) minimization stage in which the solvent molecules were minimized and the solute was restrained, followed by a second minimization in which the all the system was relaxed; b) a phase in which the system was heated from 0 to 298 K during 100 ps and afterwards subject to a c) equilibration phase for 1 ns. Equilibrated systems were simulated during 80 ns, using a timestep of 2 fs under constant pressure and temperature conditions. The SHAKE algorithm was used to constrain bonds including hydrogen atoms. Production trajectories were analyzed using the Cpptraj module of AMBER16, while energetic analyses were performed using the MMPBSA.py module [51,52]. Structural analyses were complemented using the VMD v.1.9 software [53].

Simulations were obtained using pmemd.cuda as implemented in AMBER16 using GPU computing infrastructure provided by the GPGPU Computing group at the Facultad de Matemática, Astronomía y Física (FAMAF), Universidad Nacional de Córdoba, Argentina.

2.15. Statistical analysis

The GraphPad Prism software package, version 5.00 was used for collection, processing and statistical analysis of all data. Cell viability and cell cycle assays were analyzed with two-way Analysis of Variance (ANOVA) and Bonferroni post-tests. Cell migration, adhesion, invasion and zymography assays were evaluated using one-way ANOVA and Bonferroni post-test. The p21, VDR and CYP24A1 mRNA relative levels and nuclear p27 expression were compared by unpaired *t*-test. Effects on plasma calcium levels and hematocrit of the animals were compared by unpaired *t*-test. Animal weight was analyzed by two-way ANOVA and Bonferroni post-tests. Statistical significance was determined at $p < 0.05$ level.

3. Results

3.1. EM1 induces cell cycle arrest in human T98G glioblastoma multiforme cells and does not affect human primary astrocytes viability

We had previously reported the synthesis and preliminary biological evaluation of EM1 alkynylphosphonate analogue [29]. This compound showed potent effects on the viability of various human and murine cancer cell lines and exerted an inhibitory effect on the metastatic process in a mouse model of breast cancer [32]. Regarding GBM, EM1 significantly reduced the viability of human T98G cell line (IC_{50}: 3.61×10^{-8} M) whereas calcitriol did not [29]. Taking into account this attractive result, we then proposed to continue investigating the antitumoral activity of the analogue in GBM. To this end, we started testing the effects of EM1 analogue on cell viability in other GBM cell lines (GL26 and U251) comparing its effects with that elicited by calcitriol. In addition, since most chemotherapeutic drugs used in the clinic exhibit toxicity to both normal and tumor cells, it is necessary to find compounds that display a differential action. Therefore, we also

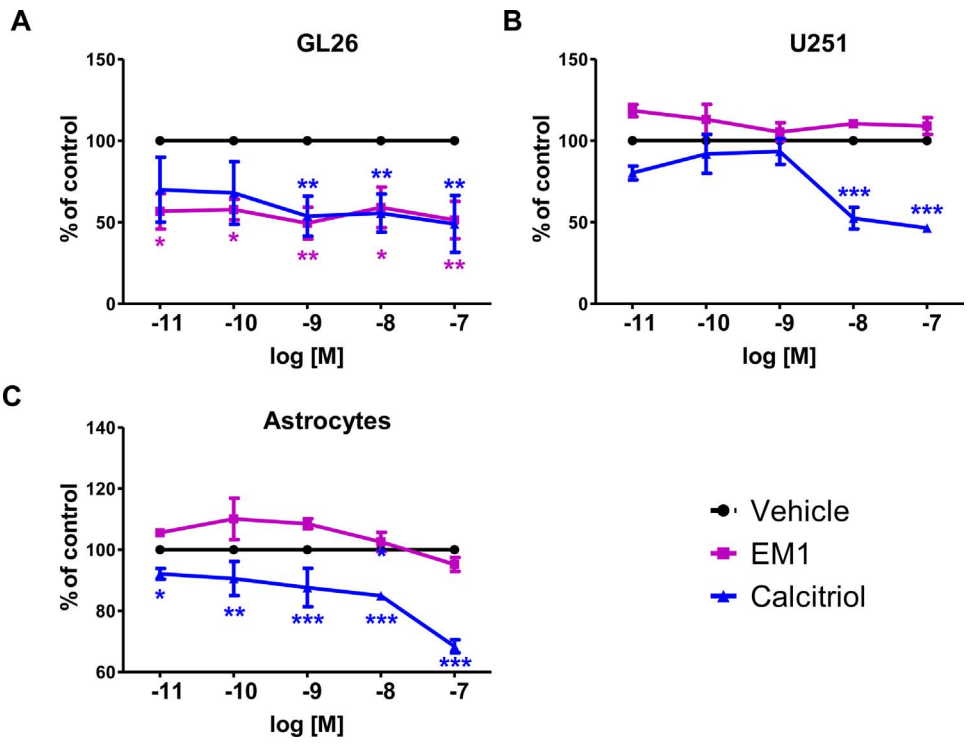

Fig. 1. Cell viability assays on A) murine GL26, B) human U251 GBM cells and C) primary astrocytes. Cells were exposed to the indicated concentrations of vehicle, EM1 or calcitriol over a total period of 120 h. Viability was expressed as percentage of the vehicle-treated cells. Data points represent the means ± SEM from two independent experiments. Two-way ANOVA and Bonferroni post-test was applied; *p < 0.05, **p < 0.01, ***p < 0.001 with respect to vehicle.

evaluated the effect of EM1 on a primary culture of human astrocytes.

As shown in Fig. 1A, both EM1 and calcitriol decreased cellular viability of the murine GL26 cell line with similar IC_{50} (EM1 = 1.38×10^{-10} M and calcitriol = 2.93×10^{-10} M). On the other hand, EM1 did not affect the viability of U251 cells whereas calcitriol significantly reduced it (IC_{50}: 5.78×10^{-9} M; Fig. 1B). Interestingly, no effect on the growth of normal human astrocytes was observed after EM1 treatment at any of the tested concentrations (0.01 to 100 nM during 120 h; Fig. 1C). Contrariwise, calcitriol reduced astrocytes viability at all concentrations tested (IC_{50}: 4.49×10^{-8} M).

All cell viability results indicate that the analogue has selectivity of action between tumor and normal cells and it is effective in reducing the viability of murine and human GBM cells. Hence, we decided to focus our attention on the effects of the analogue on human GBM cells in order to know if it has chemotherapeutic potential. Based on the previous results obtained in T98G cells [29], we further analyzed if the reduction observed in the viability of EM1-treated T98G cells was due to an effect on cell proliferation or cell death. We studied the cell cycle by flow cytometry in T98G cells treated with EM1 and labelled with PI. As depicted in Fig. 2A, analogue treatment caused an arrest in G0/G1 phase compared to vehicle-treated cells. The percentage of EM1-treated cells in G0/G1 phase was 68.43 ± 0.09% compared to 61.13 ± 0.57% in the vehicle-treated cells (**p < 0.01). No changes in the sub G0/G1 population were observed.

In order to begin to understand the molecular mechanisms underlying EM1 effects on T98G cell viability, we analyzed the expression of proteins that commonly regulate the cell cycle progression and which had been previously reported to be modulated by calcitriol treatment in other types of cancer [54]. As shown in Fig. 2B, EM1 increased the expression of the Kip/Cip family inhibitors p21, p27 and p57 that block the cell cycle through their binding to the cyclin-cdk complex. In addition, a decrease in cyclin D1 expression was observed. Furthermore, we found that the percentage of cells with nuclear p27 increased following EM1 treatment (EM1: 18.67 ± 4.04% vs vehicle: 4.13 ± 1.59%; **p < 0.01; Fig. 2C and D), suggesting its active participation in the cell cycle arrest induced by EM1. In addition, the increase in p21 expression detected by WB was confirmed by RT-qPCR (**p < 0.01; Fig. 2E).

It is well known that two important determinants of GBM tumorigenesis are the amplification and/or overexpression of epidermal growth factor receptor (EGFR) and the loss-of-function mutations of phosphatase and tensin homolog (PTEN) [55]. These alterations subsequently lead to the activation of multiple downstream signaling pathways including PI3K/Akt, RAS/RAF/MAPK pathways and their key phosphorylated kinases [56]. So, we evaluated the levels of Akt- and ERK1/2- phosphorylation in GBM cells to determine whether EM1 affects the activation of these signal transduction pathways. We found that EM1 treatment delays the phosphorylation of Akt at Ser 473 (pAkt-S473) and the phosphorylation of ERK1/2 at Thr202/Tyr204 (pERK1/2) in T98G cells (Fig. 2F). Furthermore, we found that EM1 treatment also decreases the expression of c-Jun (Fig. 2F), a nuclear transcription factor which is a downstream-substrate of MAPKs [57]. All these results are consistent with the anti-proliferative effects observed after EM1 treatment in these tumor cells. Conversely, the expression of pAkt-S473 and c-Jun did not change and the level of pERK1/2 was increased in EM1-treated U251 cells (Fig. 2F) explaining, at least partially, the lack of anti-proliferative effects of EM1 in this cell line. Altogether, these results suggest that EM1 could induce anti-proliferative effects in T98G GBM cells through an inhibition of the PI3K/Akt and RAS/RAF/MAPK pathways.

3.2. EM1 reduces the invasive behavior of GBM cells

3.2.1. Effects of EM1 on cell migration and adhesion of GBM cell lines

GBM cells are characterized by a high propensity to migrate from the primary site of tumor initiation to distant sites within the brain. This cell migration is a complex processes that includes the alteration of tumor cell adhesion to a modified extracellular matrix (ECM) [58]. Hence, we decided to evaluate the effects of the analogue on cell migration and adhesion in GBM cell lines.

On the one hand, the migratory capacity of T98G and U251 cells treated with calcitriol, EM1 or vehicle was evaluated by wound healing assays. As shown in Fig. 3A and B, EM1 demonstrated important differences in the migration process compared to the natural hormone. While EM1 significantly reduced the cellular migration of both tumor cell lines (percentage of wound closed: T98G: vehicle = 100% vs

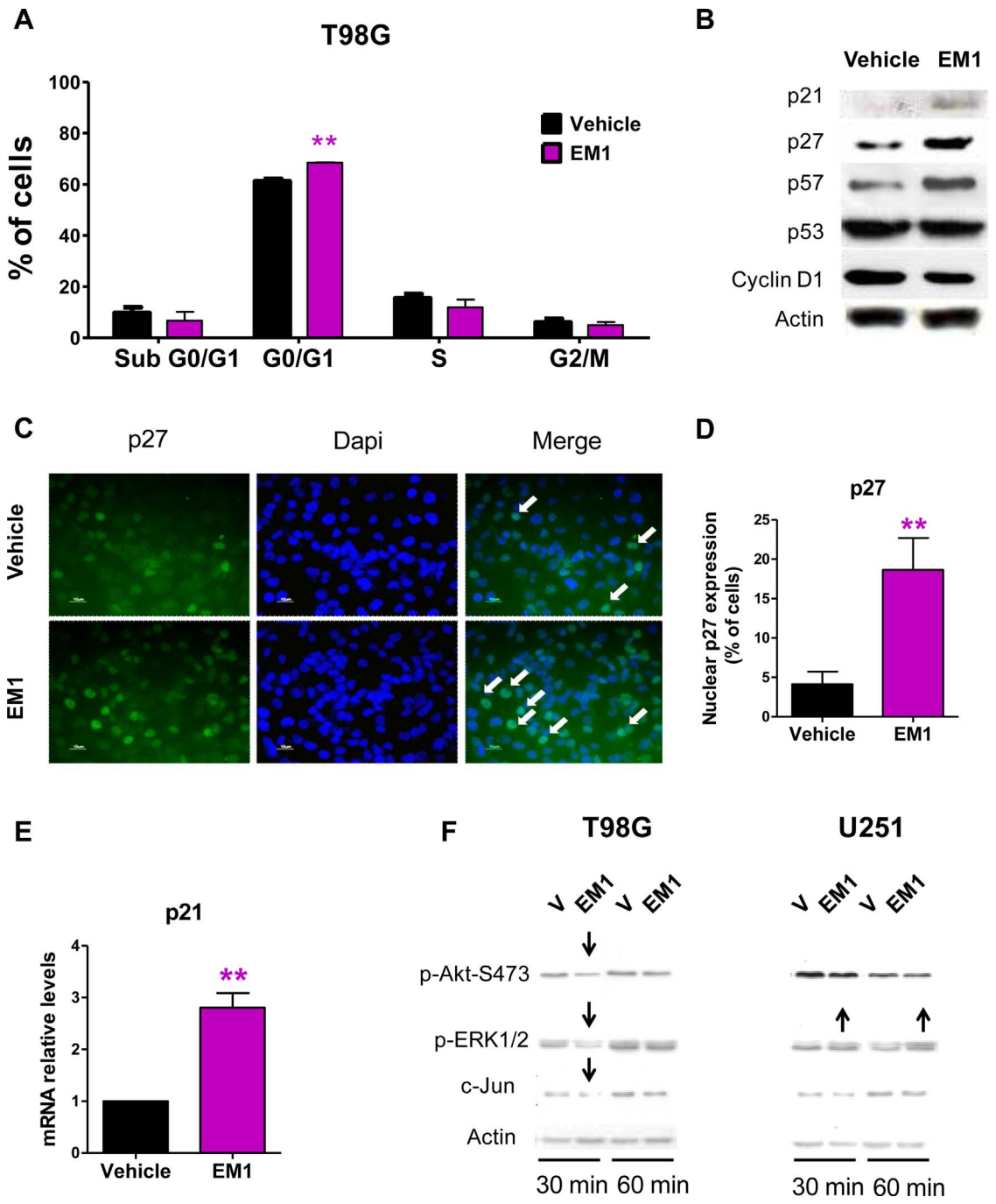

Fig. 2. Cell cycle analysis and protein expression in GBM cell lines. A) Cell cycle analysis by flow cytometry in T98G cell line treated with EM1 (100 nM, 96 h) or vehicle and stained with PI. Data points represent means ± SD from three replicates. Two-way ANOVA and Bonferroni post-test was applied; **p < 0.01. B) Effect of EM1 (100 nM, 48 h) on p21, p27, p57, p53 and cyclin D1 expression in T98G cell line. Protein loading was normalized with actin. C) Selected pictures showing p27 expression by IF in T98G cells after treatment with EM1 (100 nM, 48 h). Arrows indicate nuclear p27 localization. D) The graph shows the percentage of cells with nuclear p27 expression. Each bar represents the average of 10 randomly chosen fields. Unpaired *t*-test was applied. **p < 0.01. E) Relative levels of p21 mRNA in T98G cell line treated with EM1 (100 nM, 48 h) and vehicle. The graph shows the means ± SEM of two independent experiments. Unpaired *t*-test was applied; **p < 0.01. F) Effect of EM1 (100 nM, 30 and 60 min) or vehicle on pAkt-S473, pERK1/2 and c-Jun expression in GBM cell lines. Protein loading was normalized with actin.

EM1 = 37.26 ± 1.17%, p < 0.01; U251: vehicle = 69.63 ± 8.31% vs EM1 = 38.84 ± 4.09%, p < 0.01), calcitriol did not affect their migratory rates.

On the other hand, to evaluate the cell-substrate adhesion, GBM cells were pre-treated with calcitriol, analogue or vehicle, harvested and allowed to adhere to 96 multi-well dishes. After incubating for 30 min, the adhesive capability of both cell lines to the plastic was not altered with any treatment (Fig. 3C and D).

3.2.2. Effects of EM1 on cell invasion and MMP activity of GBM cell lines

Solid tumors, including GBM, are characterized by a profound invasion of tumor cells into the surrounding tissue [5]. Taking into account that EM1 inhibits T98G and U251 cell migration, we aimed to evaluate whether treatment with the analogue also affects the invasive capacity of GBM cells. We performed Matrigel-coated transwell invasion assays and demonstrated that the number of T98G invading cells was reduced following EM1 and calcitriol treatment (invasive cell number: EM1 = 76.75 ± 13.46, calcitriol = 83.46 ± 11.59 vs

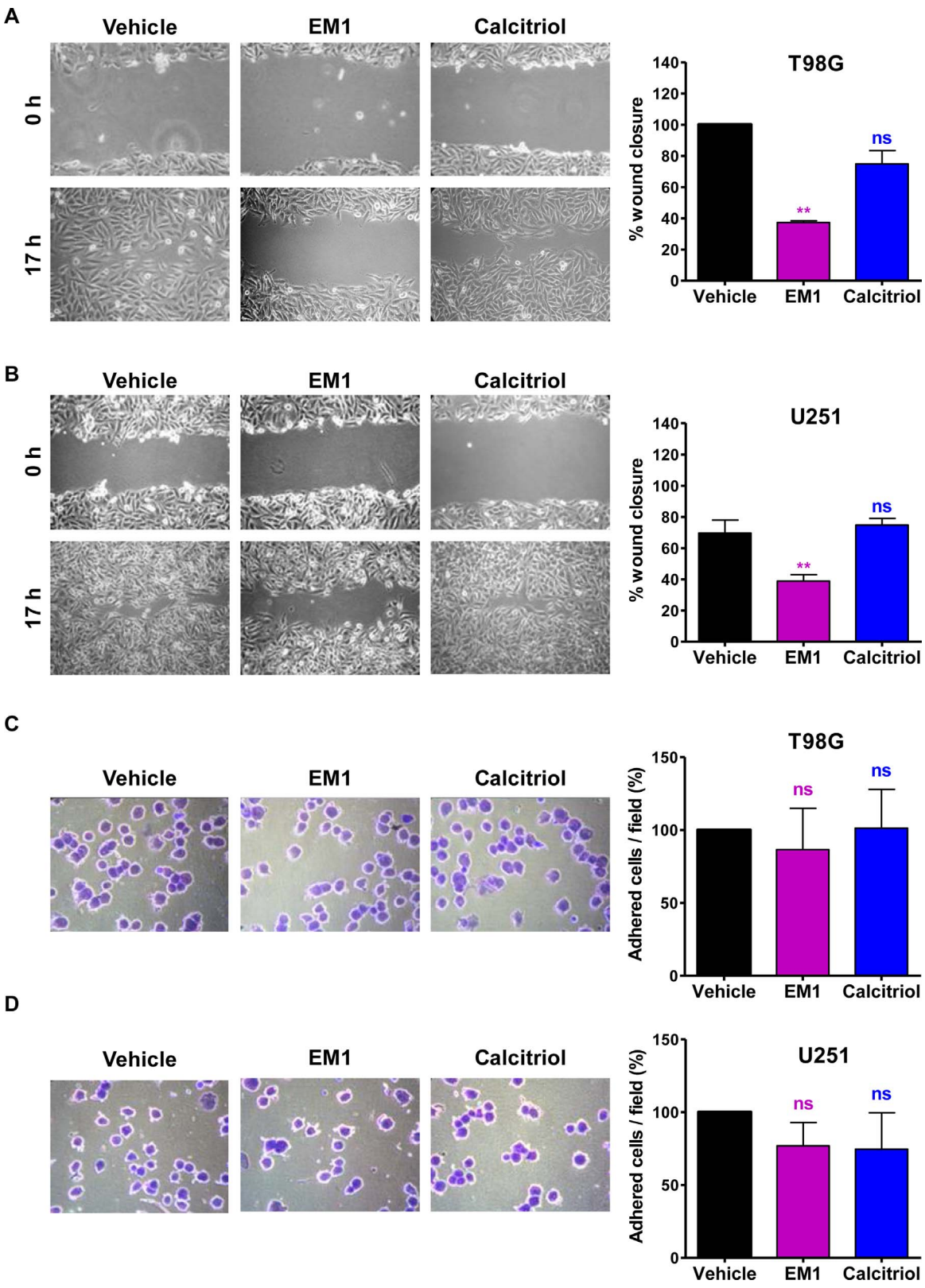

Fig. 3. Evaluation of cell migration and adhesion in GBM cell lines. A) Wound healing assays of the T98G and B) U251 cells treated with vehicle, EM1 or calcitriol (100 nM, 17 h). The cells migrating into the scratched area were photographed and the wound area was calculated as a percentage of migration respect to 0 h. C) Cell adhesion assays of T98G and D) U251 cells pre-treated with vehicle, EM1 or calcitriol (100 nM, 17 h). Following treatments and harvesting cells were allowed to adhere to 96 multi-well dishes during 30 min and attached cells were photographed after crystal violet staining. The number of adhered cells was calculated as a percentage of the vehicle-treated cells. The graphs show mean ± SEM of three independent experiments. One-way ANOVA and Bonferroni post-tests were applied. $^{**}p < 0.01$; ns: not significant. Magnification: ×200.

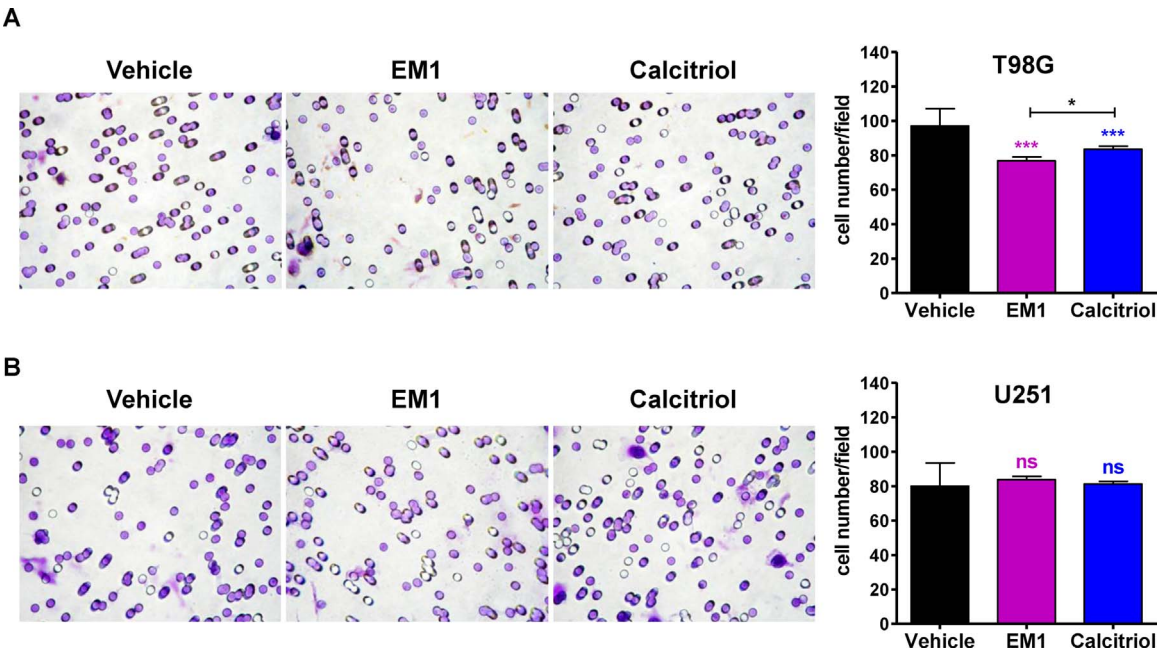

Fig. 4. Evaluation of cell invasion in GBM cell lines. Matrigel-coated transwell invasion assays were performed in A) T98G and B) U251 cells treated with vehicle, EM1 or calcitriol (100 nM, 17 h). The graphs show the mean ± SD of the number of invasive cells in each experimental condition. The assays were performed in triplicate and ten fields from each insert were counted. One-way ANOVA and Bonferroni post-tests were applied. *p < 0.05, ***p < 0.001; ns: not significant. Magnification: ×400.

vehicle = 96.97 ± 10.10; ***p < 0.001; Fig. 4A). Furthermore, EM1 produced a greater inhibitory effect than calcitriol (*p < 0.05). Regarding the invasive capacity of U251 cells, neither calcitriol nor EM1 treatment produced significant effects (Fig. 4B).

In the brain, ECM is a barrier to glioma cell invasion. To overcome this barrier, infiltrating cells secrete proteases to degrade the surrounding ECM components and generate a path through which they can invade. Among the ECM-degrading proteases, MMPs play a key role in glioma invasion [59], and particularly MMP-9 has been associated with glioma malignancy [60], so its inhibition is a potential therapeutic strategy [61]. Therefore, to explore the mechanism by which EM1 decreases the invasiveness of GBM cells, we evaluated the effect on the proteolytic activity of MMP-9 by gelatin zymography. As shown in Fig. 5A, we detected that both EM1 and calcitriol treatments decrease MMP-9 activity in T98G cells (mean of MMP-9 activity

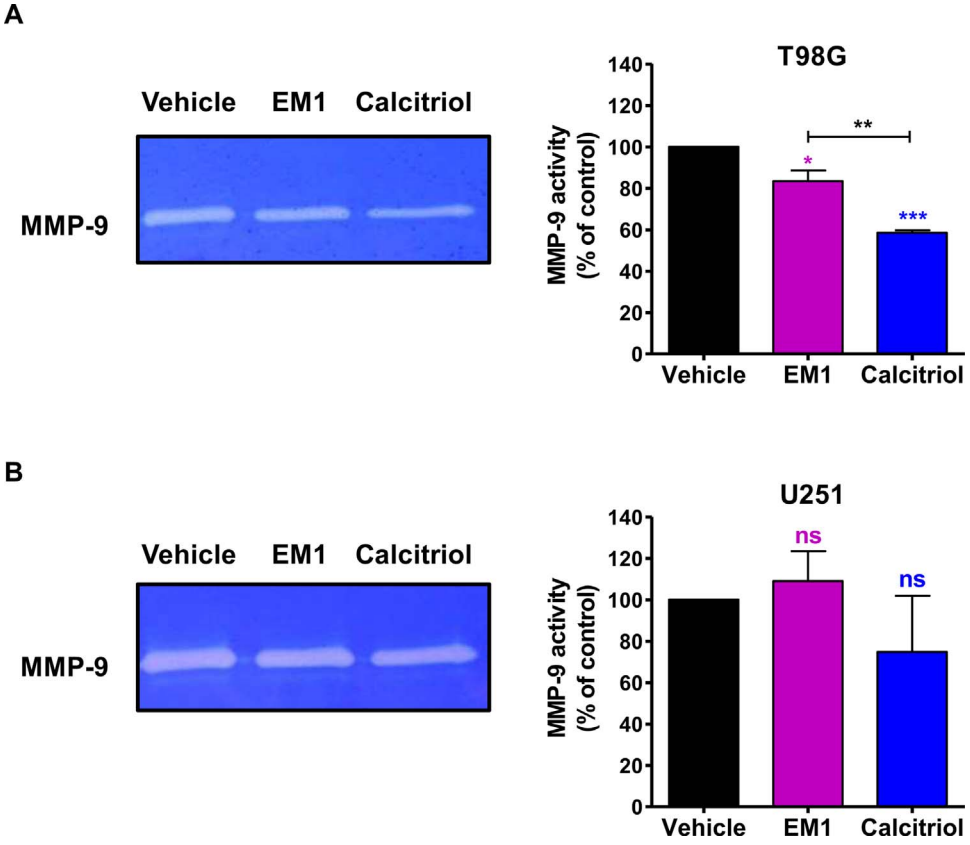

Fig. 5. Evaluation of MMP-9 proteolytic activity in GBM cell lines. A) T98G and B) U251 cells were treated with vehicle, EM1 or calcitriol (100 nM, 17 h) in serum-free medium, and their conditioned media were analyzed by zymography assay. Representative images of gelatinolytic bands are shown. The graphs indicate the mean of MMP-9 activity (expressed as percentage of control) ± SEM of three independent experiments. Data were normalized to the amount of cells/well. One-way ANOVA and Bonferroni post-tests were applied. *p < 0.05, **p < 0.01, ***p < 0.001; ns: not significant.

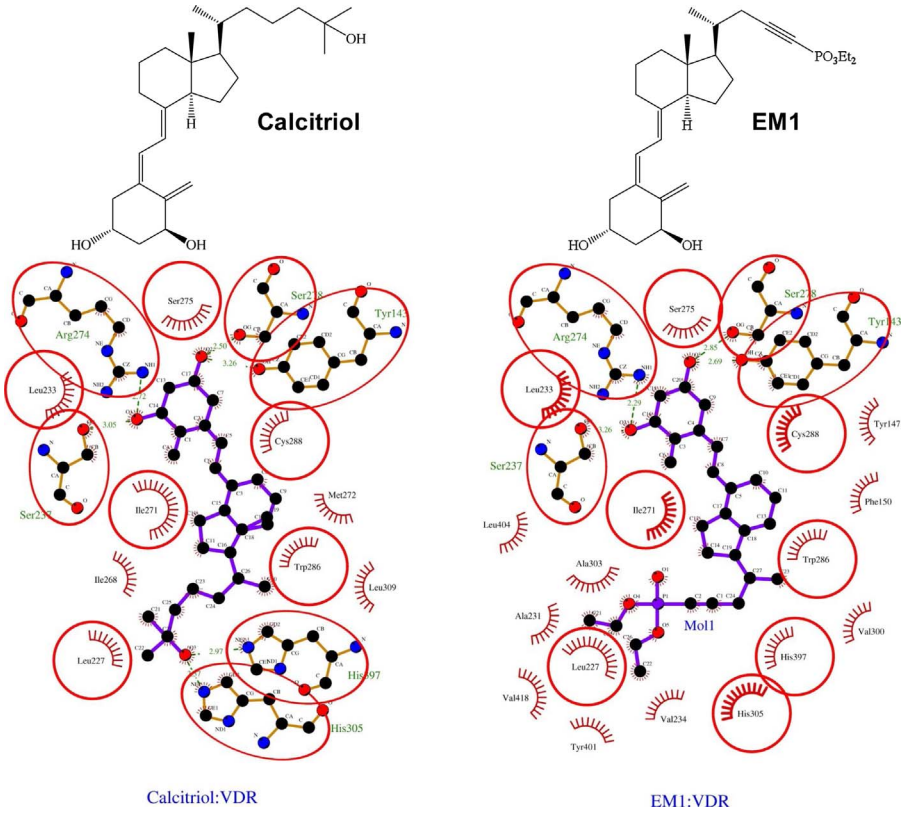

Fig. 6. Molecular docking assays. Chemical structures (upper panel) and binding of calcitriol and EM1 to VDR (lower panel). Highlighted residues correspond to shared intermolecular contacts between the analogue and calcitriol.

expressed as percentage of control: EM1 = 83.49 ± 5.07% and calcitriol = 58.56 ± 1.19% vs vehicle = 100%; *p < 0.05; ***p < 0.001 respectively). Regarding MMP-9 proteolytic activity of U251 cells, no change was observed after EM1 or calcitriol treatment (Fig. 5B). These results suggest that EM1 reduces the invasion of T98G cells, at least in part, through a decrease in MMP-9 activity.

3.3. EM1 is able to bind to the vitamin D receptor with greater affinity than calcitriol

Taking into account that calcitriol regulates numerous genes by its binding to VDR (genomic mechanism of action) and that we demonstrated that EM1 analogue modulate the expression of genes that have vitamin D response elements (VDRE) in their promoters, such as p21 and cyclin D1, Fig. 2B we conducted computational studies to evaluate if EM1 has the ability to bind to human VDR. To this end, we performed in silico assays employing human- LBD- VDR and made a comparative study of the intermolecular interaction patterns between EM1 and calcitriol. From the minimum energy docked conformations, an analogous binding mode between calcitriol and EM1 was found (Fig. 6). EM1 maintained most of the intermolecular contact established by calcitriol. These observations strongly suggest that EM1 is able to fit and efficiently interact with the calcitriol binding site in VDR. Also, additional intermolecular contacts were found for EM1, suggesting an enhanced interaction with VDR.

To further study the pharmacodynamic behavior of EM1 to VDR, the above presented complexes were subjected to MD simulations, with the corresponding interaction energies being calculated both for calcitriol and EM1 (Table 1).

As can be seen in Table 1, the total interaction energy of EM1 for VDR is higher than that of calcitriol (-80.4 and −73.5 kcal/mol, respectively), indicating a greater affinity of the modified ligand. This feature is originated on higher electrostatic and Van der Waals contacts when compared to calcitriol. When a per-residue interaction decomposition analyses was performed (Fig. 7A), it was observed that the stronger electrostatic interaction of EM1 with VDR respect to calcitriol occurs as a consequence of an enhanced electrostatic interaction of EM1 with His397, with a lesser Van der Waals contribution elicited by interaction with residues Gln230, Val234, Trp286, His305 and Tyr401.

Table 1
Overall intermolecular interaction energy components calculated for calcitriol and EM1 in their interaction with VDR.

Component	Calcitriol (kcal/mol)	EM1 (kcal/mol)
Electrostatic	−27.2	−32.7
Van der Waals	−63.5	−73.6
Total GAS	−90.8	−106.3
Non Polar Solvation	−8.4	−9.7
Polar Solvation	25.6	25.9
Total	−73.5	−80.4

In order to further assess if the binding of EM1 to VDR may elicit an allosteric activation of the AF-2 domain of VDR and thus originate the binding of transcriptional co-modulators that originates the anticancer activity [62], the RSMF values of this domain was calculated throughout the MD trajectories corresponding to calcitriol and EM1. As shown in Fig. 7B, RMSF values obtained for EM1 are comparable to those obtained for calcitriol, which in turn supports the efficient allosteric effect of the analogue on VDR activation.

3.4. EM1 up-regulates the VDR and CYP24A1 expression levels in T98G cell line

It is well known that calcitriol regulates the transcription of numerous genes including VDR and CYP24A1 [63]. In relation to VDR, the hormone is able to regulate receptor expression through VDREs located within its own enhancers [64]. Therefore, we analyzed whether the treatment with EM1 was able to modulate VDR expression levels in GBM cell lines. To this end, cells were treated with the EM1 (100 nM) and the protein levels were studied by WB. We found that EM1 induces an increase in VDR expression in T98G cells with respect to vehicle-treated cells (Fig. 8A). In contrast, no

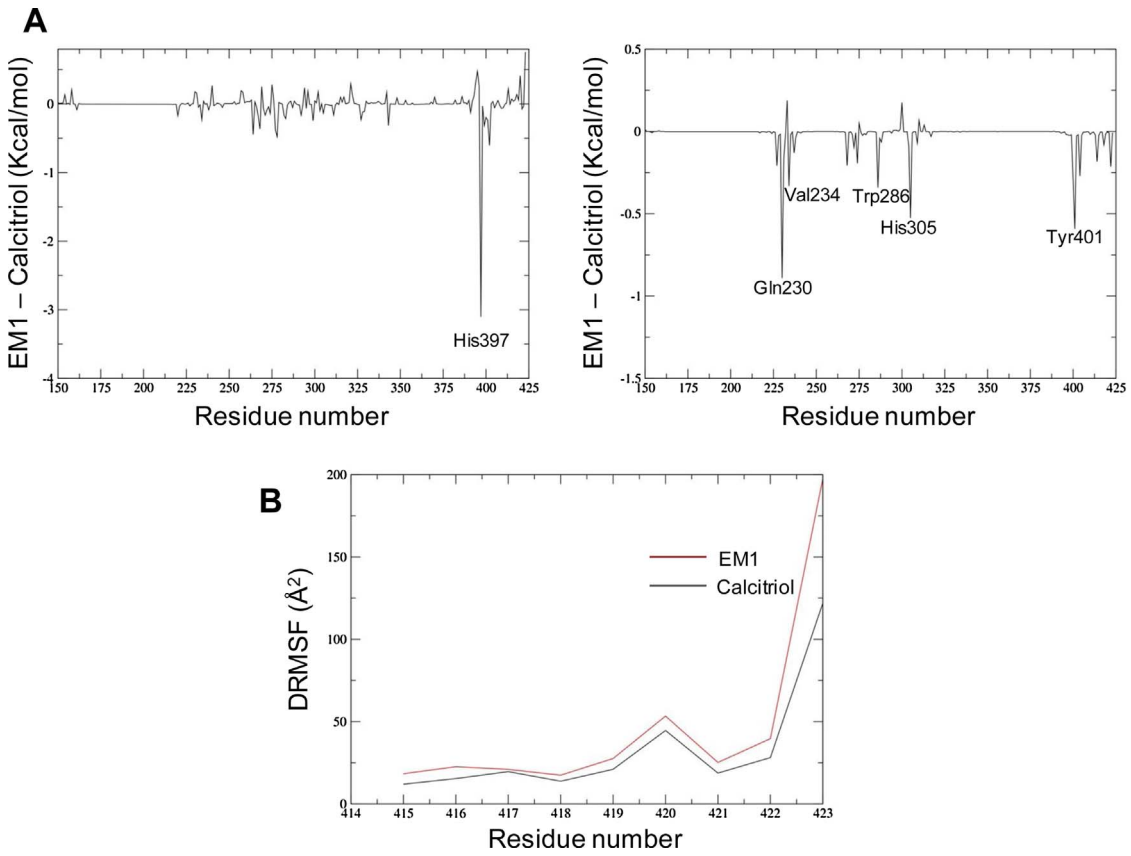

Fig. 7. MD simulations. A) Per-residue energy plot obtained for the interaction between EM1 and VDR, with the electrostatic (left) and Van der Waals (right) contributions being shown. B) RMSF plot corresponding to the AF-2 region of VDR determined from the MD trajectories when calcitriol and EM1 are bound.

differences in VDR expression were detected in U251 cells after EM1 treatment. To confirm the result obtained in T98G cells, we performed a quantification of VDR mRNA levels. As shown in Fig. 8B, the analogue significantly up-regulated VDR mRNA levels (*$p < 0.05$). CYP24A1, another gene modulated by calcitriol, encodes the 24-hydroxylase enzyme that is involved in hormone catabolism, thus limiting its antitumoral actions. Therefore, we proposed to evaluate if the analogue was also able to modulate CYP24A1 expression in T98G cells. Interestingly, we found a 129-fold up-regulation of CYP24A1 mRNA levels in EM1-treated cells (Fig. 8C). Similarly, calcitriol also increased CYP24A1 mRNA levels although it displayed a stronger effect than EM1 (589-fold vs 129-fold, **$p < 0.01$, Fig. 8C).

Preliminary experiments of our group suggested that, probably, VDR is not totally necessary for the anti-proliferative effects observed in T98G cells following EM1 treatment [29]. Taking into account that the analogue strongly reduced T98G cell migration, we decided to test if VDR was necessary for this effect. For this purpose, we employed the T98G-shVDR cell line and its control T98G-shCTRL. As shown in Fig. 8D, the analogue decreased the migration rate of T98G-shVDR cells to a lesser extent than that of the control cells (percentage of wound closed: T98G-shCTRL: vehicle = 100% vs EM1 = 45 ± 5.10%, ***$p < 0.001$; T98G-shVDR: vehicle = 100% vs EM1 = 76.67 ± 7.64%, *$p < 0.05$). This result suggests that the analogue requires the expression of the VDR to exert its effects on the migration of the T98G cell line.

3.5. EM1 does not produce hypercalcemia in N:NIH(S)-Fox1^{nu} mice administered at 50 μg/kg over 21 days

Our previous results demonstrated that the administration of EM1 to healthy CF1 mice at low doses of 5 μg/kg for a short period of time did not produce hypercalcemia, whereas calcitriol induced the adverse effects including animal death [29]. Moreover, a 15-days EM1 administration to Balb/C mice bearing mammary tumors did not result in hypercalcemia [32]. In the present work, we evaluated the effects of EM1 analogue at 50 μg/kg body weight during 21 days on the plasma calcium levels of N:NIH(S)-*Fox1^{nu}* mice, a strain of mice frequently used for xenograft implants of human GBM cell lines. We also analyzed the occurrence of toxic effects such as decreases in body weight and alterations in the hematocrit and in the liver and kidney histology of the animals. As shown in Fig. 9, EM1 did not produce hypercalcemia and the hematocrit remained within the normal levels. In addition, no changes in body weight and organs histology were found.

4. Discussion and conclusions

The standard treatment for GBM is initial surgical resection followed by chemo-radiotherapy. Despite this aggressive treatment, the outcome of patients has remained dismal [65,66] and, therefore, GBM still needs more effective therapeutic strategies. A difficulty in the research of novel chemotherapeutic drugs for GBM is the impossibility of some agents to cross the blood–brain barrier (BBB). The vitamin D endocrine system has been implicated in the prevention and treatment of various malignancies including GBM [25,67]. Specifically, calcitriol could act via binding to its corresponding receptor (VDR) to produce the antitumoral effects [7,68]. Importantly, this lipophilic hormone circulates throughout the body and crosses the BBB [69], making it an attractive therapeutic agent for GBM. However, the clinical use of this compound is limited by its side effects, mainly hypercalcemia, at the doses required to exert antitumoral effects and hence is not suitable as a chemotherapeutic agent. The current study evaluated the potential use of the novel calcitriol analogue EM1 in the treatment of GBM, and provided evidence of its chemo-sensitizing effect on GBM cells. Particularly, we demonstrated that EM1 reduces T98G cell viability by an induction of cell cycle arrest in G0/G1 phase which is accompanied by

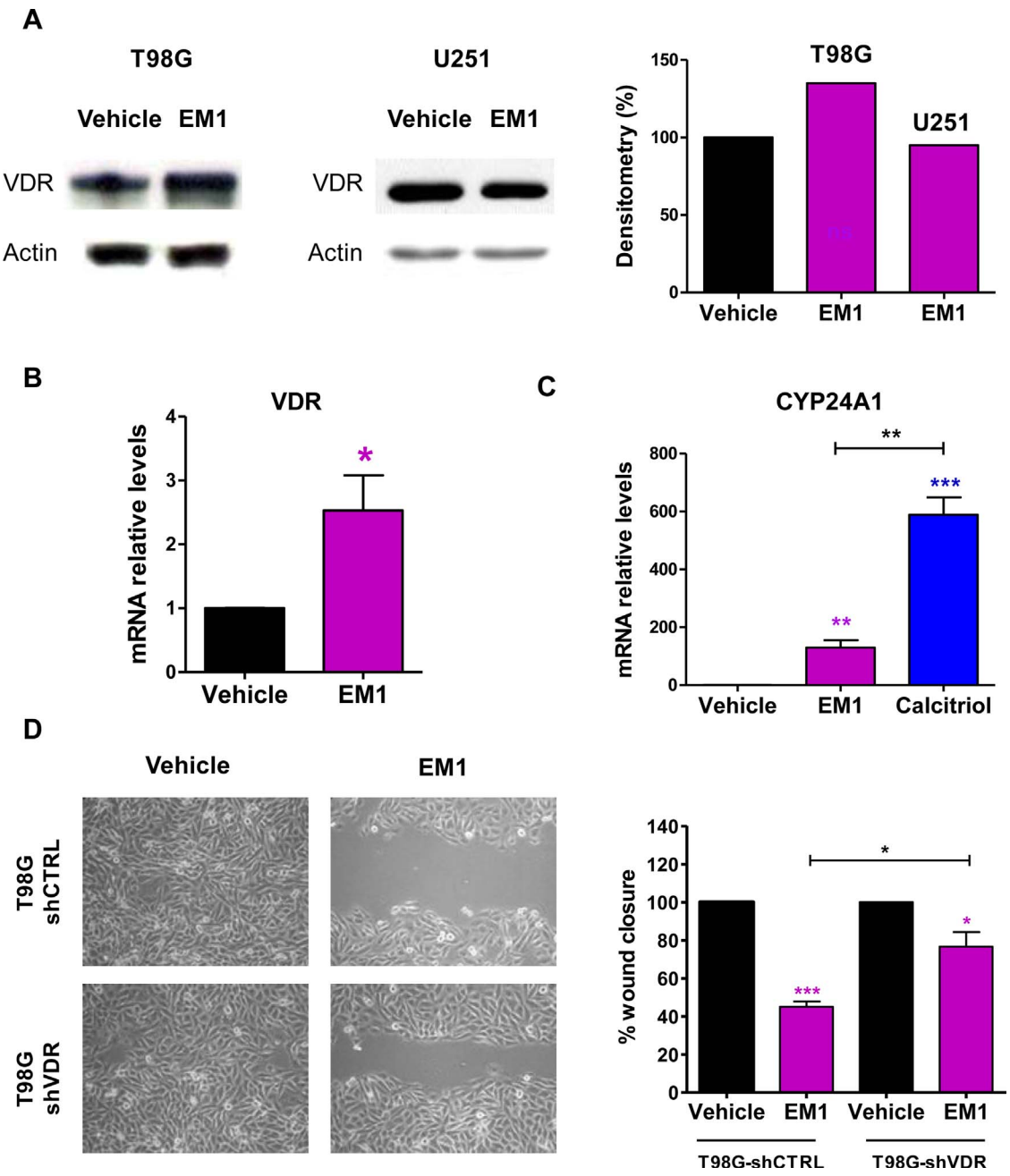

Fig. 8. VDR and CYP24A1 levels in GBM cell lines and involvement of VDR in EM1 effects on T98G cell migration. A) VDR expression levels in T98G and U251 cells treated with vehicle or EM1 (100 nM) by WB. Protein loading was normalized with actin. The blots correspond to one representative experiment. B) Relative expression of VDR mRNA in T98G cell line treated with vehicle or EM1 (100 nM). Unpaired *t*-test was applied. *p < 0.05. C) Relative expression of CYP24A1 mRNA in T98G cell line treated with vehicle, EM1 or calcitriol (100 nM). The fold change was calculated using $2^{-\Delta\Delta CT}$. The graphs show the means ± SEM from two independent experiments performed in duplicate. Unpaired *t*-test was applied. **p < 0.01, ***p < 0.001. D) Cellular migration rates in T98G-shVDR or T98G-shCTRL cells. Wound healing assays were performed in cells treated with vehicle or EM1 (100 nM, 17 h). The graph shows the mean ± SEM of three independent experiments. One-way ANOVA and Bonferroni post-tests were applied. *p < 0.05, ***p < 0.001.

up-regulation of p21, p27 and p57 and down-regulation of cyclin D1. It is well known that calcitriol activates the transcription of numerous genes such as CDKN1A (encoding p21) by binding of the complex calcitriol/VDR/RXR to VDREs [54]. So, it is possible that the analogue also up-regulates p21 expression by a similar genomic mechanism. Considering that GBM cells usually carry mutations that inactivate the apoptotic pathway [58], the enhancement of cell cycle arrest by EM1 could represent a promising strategy for the growth inhibition of GBM cells. In relation to this, the PI3K-Akt pathway is one of the most commonly hyperactivated signaling pathways in human cancer, including GBM [55,56]. Upon activation, pAkt regulates a large number of downstream substrates promoting cell cycle progression, migration, invasion, and survival as well as angiogenesis [55,70]. Particularly, pAkt promotes G1/S cell cycle progression by increasing cyclin D1 levels and through phosphorylation and impediment of nuclear import of p27 and p21 [71,72]. In this work, we demonstrated that EM1 delays Akt phosphorylation in T98G cells. In concordance with this result, we demonstrated that EM1 decreases cyclin D1 protein levels and increases those of p21 and p27. Furthermore, EM1 treatment specifically increases the nuclear localization of p27. Altogether these results demonstrate that, at least in part, the anti-proliferative effect of EM1 in T98G cells is mediated through attenuation of the PI3K/Akt pathway. Another signaling pathway that is frequently hyper-activated in GBM is RAS/RAF/MAPK pathway, which also leads to constitutive activation of

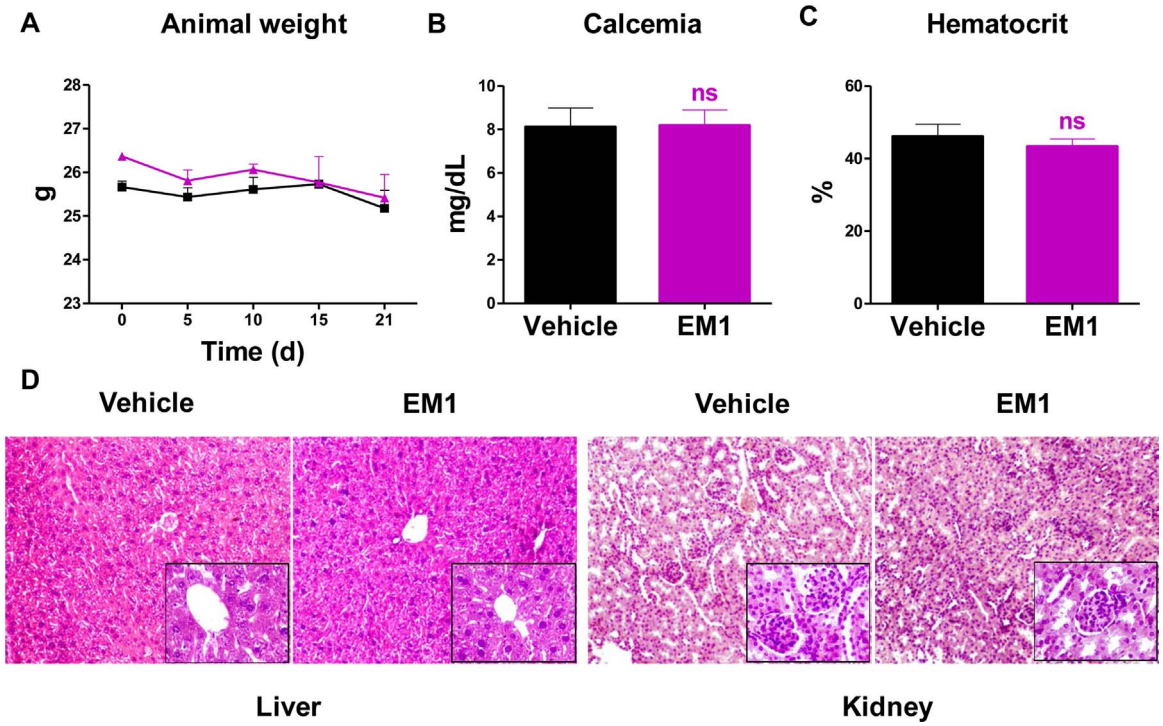

Fig. 9. Evaluation of the occurrence of calcemic and toxic effects in N:NIH(S)-*Fox1*^{nu} mice treated with EM1. A) The graph shows the mean ± SD of animal weight during the treatment period. Two-way ANOVA and Bonferroni post-test were applied. The graphs indicate the mean ± SD of B) plasma calcium levels and C) hematocrit, at the end of the treatment. Unpaired *t*-test analysis was applied. Ns: not significant. D) H & E staining of liver and kidney of one animal representative of each group. Magnification: ×100 and ×400 for the inset.

proliferation and survival signals [56]. In this work we also present evidence demonstrating that EM1 delays ERK1/2 phosphorylation and decreases the expression of c-Jun in T98G. Therefore, the attenuation of the RAS/RAF/MAPK pathway by EM1 may also explain the analogue anti-proliferative effect observed in T98G cells.

It is known that cancer cell lines display a range of sensitivities to the antitumoral effects of calcitriol and its analogues [73]. In concordance with this, our data shows that the two human GBM cell lines employed have differential sensitivity to the treatment with EM1 or calcitriol. In this context, it is important to note that the analogue demonstrated anti-proliferative effects on T98G cells which are more aggressive than the U251 cells due to their low radiation-sensitivity [74] and Temozolomide resistance [74–76]. The effects of EM1 on the arrest of the T98G-cell cycle were modest but significant; in contrast to calcitriol that did not affect viability of these cells. Therefore the analogue EM1 presents therapeutic potential to GBM cells that are resistant to conventional chemotherapy. Importantly, we found that EM1 had no effect on the viability of normal astrocytes at any of the concentration tested. Conversely, calcitriol reduced the viability of normal cells even at the lowest concentration evaluated. To our knowledge, this is the first time that the calcitriol effect on human primary astrocytes viability is reported. The difference in the response of malignant and normal cells to EM1 is of utmost importance in cancer therapeutics.

In addition to the fast growth of GBM, its highly invasive nature favors the infiltration into surrounding normal brain tissue making difficult to achieve complete tumor resection by surgery and increasing GBM recurrence [61]. Particularly, unlike other aggressive cancers that travel through the circulatory or lymphatic systems and metastasize into distant organs, high-grade gliomas rarely metastasize outside the brain but actively invade different spaces of this organ [77]. It is well known that glioma cells invasion is a multistep process that includes: adhesion of tumor cells to ECM, secretion of MMPs to degrade the local ECM and migration into the proteolytically modified ECM [60]. In this context, it is necessary that new treatment options for GBM not only target cell proliferation but also suppress its highly invasive phenotype. Therefore, in the present work, in addition to demonstrating that EM1 decreases the viability of GBM T98G cells by inducing cell cycle arrest, we also evaluated its effect on the multi-step process of GBM local invasion. On the one hand, we demonstrated that EM1 decreases the migratory capability of both GBM cells lines, T98G and U251. This effect was not mediated by changes in the adhesion of tumor cells to the substrate. In contrast to EM1, calcitriol did not exert anti-migratory activity on any of the GBM cell lines. On the other hand, we found that EM1 reduces MMP-9 activity in the T98G cell line, while no effect was detected in U251 cells. All these results, explain at least in part, the anti-invasive effect of the analogue detected in T98G GBM cells. Importantly, similar to what occurs at the level of cell proliferation, EM1 suppresses the invasive phenotype of the most aggressive and less responsive to conventional treatment T98G cell line.

Vitamin D Receptor (VDR) has been demonstrated to be useful as a prognostic factor for some types of cancer and, particularly in GBM, VDR expression is associated with an improved outcome of the patients [25]. In this regard, the identification of compounds that increase the expression of VDR can be useful in the treatment of these pathologies. Our results demonstrated an up-regulation of VDR with EM1 in T98G cells. Moreover, our computational studies of the interaction between EM1 and VDR demonstrated that the analogue is able to bind to the LBD- VDR, and also exhibits an enhanced affinity compared to calcitriol. The in silico results indicated the establishment of significant electrostatic interactions between the phosphate group present in this ligand and His397 of VDR and additional Van der Waals interactions that further enhanced the affinity of EM1 for VDR. We had previously demonstrated no alteration in the cellular count following EM1 treatment of T98G cells when VDR was partially knockdown [29], suggesting that the effect of EM1 could be VDR − independent. However, it is possible that the small amount of VDR present in the silenced cells is sufficient to mediate the effects of EM1 on decreasing cell viability. In addition, as EM1 was designed to be poorly metabolized, its high levels may be enough to bind to the low levels of VDR to exert the anti-proliferative and anti-migratory effects.

On the other hand, it has been reported that astrocytes and glioma cells have high levels of CYP24A1 [21,78]. The augmented expression of CYP24A1 has been shown to be detrimental to calcitriol anti-proliferative effects. For example, in prostate cancer cell lines, it has been demonstrated that enzyme expression was inversely correlated to the anti-proliferative effects displayed by the cells [79]. Our results showed that both EM1 and calcitriol induce up-regulation of CYP24A1 in T98G cells, although the natural hormone exerts a stronger effect. The fact that EM1 bears a C24 triple bond in its side chain makes it less prone to degradation by the CYP24A1 enzyme and this may account for the strong antitumoral effects of the analogue. Since supraphysiological doses of calcitriol are required to elicit antitumoral effects, the chemical structure of EM1 probably accounts for the activity of the analogue at much lower concentrations than calcitriol.

In conclusion, EM1 displays anti-proliferative, anti-migratory and anti-invasive activity against T98G cells, an aggressive and low chemo-radiotherapy- sensitive GBM cell line. These antitumoral effects are mediated, at least in part, through attenuation of the PI3K/Akt and RAS/MAPK pathways followed by the subsequent modulation of cell cycle regulators, and a reduction in MMP-9 activity. Moreover, EM1 does not affect the viability of human primary astrocytes and does not exert hypercalcemic effects in mice. All the results make EM1 an attractive antitumoral drug candidate for GBM treatment.

Conflict of interest

The authors declare no conflicts of interest.

Acknowledgements

This work was supported by the Agencia Nacional de Promoción Científica y Tecnológica (ANPCyT, PICTs 2007-1797 and 2012-0966), Consejo Nacional de Investigaciones Científicas y Técnicas (CONICET, PIP 112-201101-00556) and by Universidad Nacional del Sur, Bahía Blanca, Buenos Aires, Argentina (PGI 24/B174). María J. Ferronato, Eliana N. Alonso, Débora G. Salomón were recipients of a fellowship from CONICET. We thank Dr. Julián Arévalo for kindly analyzing the histological slides and Dr. Tokino T. from the Sapporo Medical University (Japan) for providing pFIV-H1-Puro shRNA VDR plasmids. The authors would also like to thank the GPGPU Computing Group from the Facultad de Matemática, Astronomía y Física (FAMAF), Universidad Nacional de Córdoba, Argentina, for providing access to computing resources. Mario A. Quevedo wishes to thank OpenEye Scientific Software and their Free Academic Licensing program for providing him with licenses to use the corresponding software packages.

References

[1] J. Shi, B. Dong, J. Cao, Y. Mao, W. Guan, Y. Peng, S. Wang, Long non-coding RNA in glioma: signaling pathways, Oncotarget 8 (16) (2017) 27582, , http://dx.doi.org/10.18632/oncotarget.15175.

[2] M. Zorzan, E. Giordan, M. Redaelli, A. Caretta, C. Mucignat-Caretta, Molecular targets in glioblastoma, Future Oncol. 11 (9) (2015) 1407–1420, http://dx.doi.org/10.2217/fon.15.22.

[3] H.G. Wirsching, M. Weller, Glioblastoma, Handb. Clin. Neurol. 134 (2016) 381–397, http://dx.doi.org/10.1016/B978-0-12-802997-8.00023-2.

[4] S.S. Kim, J.B. Harford, K.F. Pirollo, E.H. Chang, Effective treatment of glioblastoma requires crossing the blood–brain barrier and targeting tumors including cancer stem cells: the promise of nanomedicine, Biochem. Biophys. Res. Commun. 468 (3) (2015) 485–489, http://dx.doi.org/10.1016/j.bbrc.2015.06.137.

[5] M. Jhanwar-Uniyal, M. Labagnara, M. Friedman, A. Kwasnicki, R. Murali, Glioblastoma: molecular pathways, stem cells and therapeutic targets, Cancers 7 (2) (2015) 538–555, http://dx.doi.org/10.3390/cancers7020538.

[6] L. Díaz, M. Díaz-Muñoz, A.C. García-Gaytán, I. Méndez, Mechanistic effects of calcitriol in cancer biology, Nutrients 7 (6) (2015) 5020–5050, http://dx.doi.org/10.3390/nu7065020.

[7] B.B. Merchan, S. Morcillo, G. Martin-Nuñez, F.J. Tinahones, M. Macías-González, The role of vitamin D and VDR in carcinogenesis: through epidemiology and basic sciences, J. Steroid Biochem. Mol. Biol. (2016), http://dx.doi.org/10.1016/j.jsbmb.2016.11.020.

[8] D. Hanahan, R.A. Weinberg, Hallmarks of cancer: the next generation, Cell 144 (5) (2011) 646–674, http://dx.doi.org/10.1016/j.cell.2011.02.013.

[9] D.G. Salomón, E. Mascaro, S.M. Grioli, M.J. Ferronato, C.A. Vitale, G.E. Radivoy, et al., Phosphonate analogues of 1α, 25 dihydroxyvitamin D3 are promising candidates for antitumoural therapies, Curr. Top. Med. Chem. 14 (21) (2014) 2408–2423, http://dx.doi.org/10.2174/1568026615666141208101418.

[10] F. Pereira, M.J. Larriba, A. Muñoz, Vitamin D and colon cancer, Endocr. Relat. Cancer 19 (3) (2012) R51–R71, http://dx.doi.org/10.1530/ERC-11-0388.

[11] J. Welsh, Cellular and molecular effects of vitamin D on carcinogenesis, Arch. Biochem. Biophys. 523 (1) (2012) 107–114, http://dx.doi.org/10.1016/j.abb.2011.10.019.

[12] I. Orlov, N. Rochel, D. Moras, B.P. Klaholz, Structure of the full human RXR/VDR nuclear receptor heterodimer complex with its DR3 target DNA, EMBO J. 31 (2) (2012) 291–300, http://dx.doi.org/10.1038/emboj.2011.445.

[13] F.C. Campbell, H. Xu, M. El-Tanani, P. Crowe, V. Bingham, The yin and yang of vitamin D receptor (VDR) signaling in neoplastic progression: operational networks and tissue-specific growth control, Biochem. Pharmacol. 79 (1) (2010) 1–9, http://dx.doi.org/10.1016/j.bcp.2009.09.005.

[14] L. Magrassi, G. Butti, S. Pezzotta, L. Infuso, G. Milanesi, Effects of vitamin D and retinoic acid on human glioblastoma cell lines, Acta Neurochir. 133 (3) (1995) 184–190, http://dx.doi.org/10.1007/BF01420072.

[15] L. Magrassi, L. Adorni, G. Montorfano, S. Rapelli, G. Butti, B. Berra, G. Milanesi, Vitamin D metabolites activate the sphingomyelin pathway and induce death of glioblastoma cells, Acta Neurochir. 140 (7) (1998) 707–714, http://dx.doi.org/10.1007/s007010050166.

[16] C. Baudet, G. Chevalier, P. Naveilhan, L. Binderup, P. Brachet, D. Wion, Cytotoxic effects of 1α, 25-dihydroxyvitamin D3 and synthetic vitamin D3 analogues on a glioma cell line, Cancer Lett. 100 (1–2) (1996) 3–10, http://dx.doi.org/10.1016/0304-3835(95)04054-4.

[17] C. Baudet, G. Chevalier, A. Chassevent, C. Canova, R. Filmon, F. Larra, et al., 1, 25-Dihydroxyvitamin D3 induces programmed cell death in a rat glioma cell line, J. Neurosci. Res. 46 (5) (1996) 540–550, http://dx.doi.org/10.1002/(SICI)1097-4547(19961201)46:5<540::AID-JNR3>3.0.CO;2-J.

[18] N. Davoust, D. Wion, G. Chevalier, M. Garabedian, P. Brachet, D. Couez, Vitamin D receptor stable transfection restores the susceptibility to 1, 25-dihydroxyvitamin D3cytotoxicity in a rat glioma resistant clone, J. Neurosci. Res. 52 (2) (1998) 210–219, http://dx.doi.org/10.1002/(SICI)1097-4547(19980415)52:2<210::AID-JNR9>3.0.CO;2-D.

[19] P. Naveilhan, F. Berger, K. Haddad, N. Barbot, A.L. Benabid, P. Brachet, D. Wion, Induction of glioma cell death by 1, 25 (OH) 2 vitamin D3: towards an endocrine therapy of brain tumors? J. Neurosci. Res. 37 (2) (1994) 271–277, http://dx.doi.org/10.1002/jnr.490370212.

[20] J. Zou, H. Landy, L. Feun, R. Xu, T. Lampidis, C.J. Wu, et al., Correlation of a unique 220-kDa protein with vitamin D sensitivity in glioma cells, Biochem. Pharmacol. 60 (9) (2000) 1361–1365, http://dx.doi.org/10.1016/S0006-2952(00)00438-X.

[21] B. Diesel, J. Radermacher, M. Bureik, R. Bernhardt, M. Seifert, J. Reichrath, et al., Vitamin D3 metabolism in human glioblastoma multiforme: functionality of CYP27B1 splice variants, metabolism of calcidiol, and effect of calcitriol, Clin. Cancer Res. 11 (15) (2005) 5370–5380, http://dx.doi.org/10.1158/1078-0432.

[22] X. Chen, C. Wang, L. Teng, Y. Liu, X. Chen, G. Yang, et al., Calcitriol enhances 5-aminolevulinic acid-induced fluorescence and the effect of photodynamic therapy in human glioma, Acta Oncol. 53 (3) (2014) 405–413, http://dx.doi.org/10.3109/0284186X.2013.819993.

[23] D.H. Bak, S.H. Kang, D.R. Choi, M.N. Gil, K.S. Yu, J.H. Jeong, et al., Autophagy enhancement contributes to the synergistic effect of vitamin D in temozolomide-based glioblastoma chemotherapy, Exp. Ther. Med. 11 (6) (2016) 2153–2162, http://dx.doi.org/10.3892/etm.2016.3196.

[24] S. Reichrath, C.S. Müller, B. Gleissner, M. Pfreundschuh, T. Vogt, J. Reichrath, Notch-and vitamin d signaling in 1, 25 (OH) 2 D 3-resistant glioblastoma multiforme (GBM) cell lines, J. Steroid Biochem. Mol. Biol. 121 (1) (2010) 420–424, http://dx.doi.org/10.1016/j.jsbmb.2010.02.028.

[25] D.G. Salomón, M.E. Fermento, N.A. Gandini, M.J. Ferronato, J. Arévalo, J. Blasco, et al., Vitamin D receptor expression is associated with improved overall survival in human glioblastoma multiforme, J. Neurooncol. 118 (1) (2014) 49–60, http://dx.doi.org/10.1007/s11060-014-1416-3.

[26] J.L. Osborn, G.G. Schwartz, D.C. Smith, R. Bahnson, R. Day, D.L. Trump, Phase II trial of oral 1, 25-dihydroxyvitamin D (calcitriol) in hormone refractory prostate cancer, Urol. Oncol. 1 (1995) 195–198, http://dx.doi.org/10.1016/1078-1439(95)00061-5.

[27] A. Woloszynska-Read, C.S. Johnson, D.L. Trump, Vitamin D and cancer: clinical aspects, Best Pract. Res. Clin. Endocrinol. Metab. 25 (4) (2011) 605–615, http://dx.doi.org/10.1016/j.beem.2011.06.006.

[28] W. Luo, P.A. Hershberger, D.L. Trump, C.S. Johnson, 24-Hydroxylase in cancer: impact on vitamin D-based anticancer therapeutics, J. Steroid Biochem. Mol. Biol. 136 (2013) 252–257, http://dx.doi.org/10.1016/j.jsbmb.2012.09.031.

[29] D.G. Salomón, S.M. Grioli, M. Buschiazzo, E. Mascaró, C. Vitale, G. Radivoy, et al., Novel alkynylphosphonate analogue of calcitriol with potent antiproliferative effects in cancer cells and lack of calcemic activity, ACS Med. Chem. Lett. 2 (7) (2011) 503–508, http://dx.doi.org/10.1021/ml200034w.

[30] A. Steinmeyer, K. Schwarz, M. Haberey, G. Langer, H. Wiesinger, Synthesis and biological activities of a new series of secosteroids: vitamin D phosphonate hybrids, Steroids 66 (3) (2001) 257–266, http://dx.doi.org/10.1016/S0039-128X(00)00148-3.

[31] M.R. Uskokovic, A.W. Norman, P.S. Manchand, G.P. Studzinski, M.J. Campbell, H.P. Koeffler, et al., Highly active analogs of 1α, 25-dihydroxyvitamin D 3 that resist metabolism through C-24 oxidation and C-3 epimerization pathways, Steroids

66 (3) (2001) 463–471, http://dx.doi.org/10.1016/S0039-128X(00)00226-9.
[32] M.J. Ferronato, D.J. Obiol, M.E. Fermento, N.A. Gandini, E.N. Alonso, D.G. Salomón, et al., The alkynylphosphonate analogue of calcitriol EM1 has potent anti-metastatic effects in breast cancer, J. Steroid Biochem. Mol. Biol. 154 (2015) 285–293, http://dx.doi.org/10.1016/j.jsbmb.2015.09.009.
[33] E.N. Alonso, M.J. Ferronato, N.A. Gandini, M.E. Fermento, D.J. Obiol, López Romero, et al., Antitumoral effects of D-fraction from grifola frondosa (Maitake) mushroom in breast cancer, Nutr. Cancer 69 (1) (2017) 29–43, http://dx.doi.org/10.1080/01635581.2017.1247891.
[34] K.J. Livak, T.D. Schmittgen, Analysis of relative gene expression data using real-time quantitative PCR and the 2-ΔΔCT method, Methods 25 (4) (2001) 402–408, http://dx.doi.org/10.1016/j.jsbmb.2012.09.031.
[35] N. Rochel, J.M. Wurtz, A. Mitschler, B. Klaholz, D. Moras, The crystal structure of the nuclear receptor for vitamin D bound to its natural ligand, Mol. Cell 5 (1) (2000) 173–179, http://dx.doi.org/10.1016/S1097-2765(00)80413-X.
[36] M. Malinska, A. Kutner, K. Woźniak, Predicted structures of new Vitamin D Receptor agonists based on available X-ray structures, Steroids 104 (2015) 220–229, http://dx.doi.org/10.1016/j.steroids.2015.10.007.
[37] MarvinSketch v.6.31, ChemAxon Ltd., http://www.chemaxon.com.
[38] M.J. Frisch, G.W. Trucks, H.B. Schlegel, G.E. Scuseria, M.A. Robb, J.R. Cheeseman, J.A. Montgomery, et al., Gaussian 03, Gaussian, Inc., 2003.
[39] OpenEye. Scientific.Software, Santa Fe, NM, http://www.eyesopen.com.
[40] Omega.2.4.3. OpenEye Scientific Software, Santa Fe, NM http://www.eyesopen.com.
[41] P.C. Hawkins, A.G. Skillman, G.L. Warren, B.A. Ellingson, M.T. Stahl, Conformer generation with OMEGA: algorithm and validation using high quality structures from the Protein Databank and Cambridge Structural Database, J. Chem. Inf. Model. 50 (4) (2010) 572–584, http://dx.doi.org/10.1021/ci100031x.
[42] Fred.3.0.0 OpenEye.Scientific.Software, Santa Fe, NM, http://www.eyesopen.com.
[43] M. McGann, FRED and HYBRID docking performance on standardized datasets, J. Comput. Aided Mol. Des. 26 (8) (2012) 897–906, http://dx.doi.org/10.1007/s10822-012-9584-8.
[44] M. McGann, FRED pose prediction and virtual screening accuracy, J. Chem. Inf. Model. 51 (3) (2011) 578–596, http://dx.doi.org/10.1021/ci100436p.
[45] VIDA.4.2.1. OpenEye Scientific Software, Santa Fe, NM http://www.eyesopen.com.
[46] R.A. Laskowski, M.B. Swindells, LigPlot+: multiple ligand–protein interaction diagrams for drug discovery, J. Chem. Inf. Model. 51 (10) (2011) 2778–2786, http://dx.doi.org/10.1021/ci200227u.
[47] D.A. Case, T.E. Cheatham, T. Darden, H. Gohlke, R. Luo, K.M. Merz, et al., The Amber biomolecular simulation programs, J. Comput. Chem. 26 (16) (2005) 1668–1688, http://dx.doi.org/10.1002/jcc.20290.
[48] R. Salomon-Ferrer, D.A. Case, R.C. Walker, An overview of the Amber biomolecular simulation package, Wiley Interdisc. Rev. Comput. Mol. Sci. 3 (2) (2013) 198–210, http://dx.doi.org/10.1002/wcms.1121.
[49] J. Wang, R.M. Wolf, J.W. Caldwell, P.A. Kollman, D.A. Case, Development and testing of a general amber force field, J. Comput. Chem. 25 (9) (2004) 1157–1174, http://dx.doi.org/10.1002/jcc.20035.
[50] J.A. Maier, C. Martinez, K. Kasavajhala, L. Wickstrom, K.E. Hauser, C. Simmerling, ff14SB: improving the accuracy of protein side chain and backbone parameters from ff99SB, J. Chem. Theory Comput. 11 (8) (2015) 3696–3713, http://dx.doi.org/10.1021/acs.jctc.5b00255.
[51] B. Kuhn, P. Gerber, T. Schulz-Gasch, M. Stahl, Validation and use of the MM-PBSA approach for drug discovery, J. Med. Chem. 48 (12) (2005) 4040–4048, http://dx.doi.org/10.1021/jm049081q.
[52] B.R. Miller, T.D. McGee Jr., J.M. Swails, N. Homeyer, H. Gohlke, A.E. Roitberg, MMPBSA. py: an efficient program for end-state free energy calculations, J. Chem. Theory Comput. 8 (9) (2012) 3314–3321, http://dx.doi.org/10.1021/ct300418h.
[53] W. Humphrey, A. Dalke, K. Schulten, VMD-visual molecular dynamics, J. Mol. Graph. 14 (1996) 33–38, http://dx.doi.org/10.1016/0263-7855(96)00018-5.
[54] L. Vuolo, A. Faggiano, A.A. Colao, Vitamin D and cancer, Front. Endocrinol. 3 (2012) 58, http://dx.doi.org/10.3389/fendo.2012.00058.
[55] X. Li, C. Wu, N. Chen, H. Gu, A. Yen, L. Cao, et al., PI3K/Akt/mTOR signaling pathway and targeted therapy for glioblastoma, Oncotarget 7 (22) (2016) 33440–33450, http://dx.doi.org/10.18632/oncotarget.7961.
[56] Q. Gao, T. Lei, F. Ye, Therapeutic targeting of EGFR-activated metabolic pathways in glioblastoma, Expert Opin. Investig. Drugs 22 (8) (2013) 1023–1040, http://dx.doi.org/10.1517/13543784.2013.806484.
[57] Z. Deng, G. Sui, P.M. Rosa, W. Zhao, Radiation-induced c-Jun activation depends on MEK1-ERK1/2 signaling pathway in microglial cells, PLoS One 7 (5) (2012) e36739, , http://dx.doi.org/10.1371/journal.pone.0036739.
[58] F. Lefranc, J. Brotchi, R. Kiss, Possible future issues in the treatment of glioblastomas: special emphasis on cell migration and the resistance of migrating glioblastoma cells to apoptosis, J. Clin. Oncol. 23 (10) (2005) 2411–2422, http://dx.doi.org/10.1200/JCO.2005.03.089.
[59] M. Nakada, Y. Okada, J. Yamashita, The role of matrix metalloproteinases in glioma invasion, Front. Biosci. J. Virt. Libr. 8 (2003) e261–e269, http://dx.doi.org/10.2741/1016.
[60] Y. Suzuki, K. Fujioka, K. Ikeda, Y. Murayama, Y. Manome, Temozolomide does not influence the transcription or activity of matrix metalloproteinases 9 and 2 in glioma cell lines, J. Clin. Neurosci. 41 (2017) 144–149, http://dx.doi.org/10.1016/j.jocn.2017.03.048.
[61] J.S. Rao, Molecular mechanisms of glioma invasiveness: the role of proteases, Nat. Rev. Cancer 3 (7) (2003) 489, http://dx.doi.org/10.1038/nrc1121.
[62] T. Huet, G. Laverny, F. Ciesielski, F. Molnár, T.G. Ramamoorthy, A.Y. Belorusova, et al., A vitamin D receptor selectively activated by gemini analogs reveals ligand dependent and independent effects, Cell Rep. 10 (4) (2015) 516–526, http://dx.doi.org/10.1016/j.celrep.2014.12.045.
[63] M.R. Haussler, G.K. Whitfield, I. Kaneko, C.A. Haussler, D. Hsieh, J.C. Hsieh, P.W. Jurutka, Molecular mechanisms of vitamin D action, Calcif. Tissue Int. 92 (2) (2013) 77–98, http://dx.doi.org/10.1007/s00223-012-9619-0.
[64] L.A. Zella, S. Kim, N.K. Shevde, J.W. Pike, Enhancers located in the vitamin D receptor gene mediate transcriptional autoregulation by 1, 25-dihydroxyvitamin D 3, J. Steroid Biochem. Mol. Biol. 103 (3) (2007) 435–439, http://dx.doi.org/10.1016/j.jsbmb.2006.12.019.
[65] R. Chen, A.L. Cohen, H. Colman, Targeted therapeutics in Patients with high-grade gliomas: past, present, and future, Curr. Treat. Options Oncol. 17 (8) (2016) 1–11, http://dx.doi.org/10.1007/s11864-016-0418-0.
[66] R. Stupp, S. Taillibert, A.A. Kanner, S. Kesari, D.M. Steinberg, S.A. Toms, et al., Maintenance therapy with tumor-treating fields plus temozolomide vs temozolomide alone for glioblastoma: a randomized clinical trial, JAMA 314 (23) (2015) 2535–2543, http://dx.doi.org/10.1001/jama.2015.16669.
[67] Mulpur, B.H., Nabors, L.B., Thompson, R.C., Olson, J.J., LaRocca, R.V., Thompson, Z., Egan, K.M. (2015). Complementary therapy and survival in glioblastoma. Neurooncol. Pract. npv008. doi: 10.1093/nop/npv008.
[68] M.J. Duffy, A. Murray, N.C. Synnott, N. O'Donovan, J. Crown, Vitamin D analogues: potential use in cancer treatment, Crit. Rev. Oncol. Hematol. 112 (2017) 190–197, http://dx.doi.org/10.1016/j.critrevonc.2017.02.015.
[69] L.R. Harms, T.H. Burne, D.W. Eyles, J.J. McGrath, Vitamin D and the brain, Best Pract. Res. Clin. Endocrinol. Metab. 25 (4) (2011) 657–669, http://dx.doi.org/10.1016/j.beem.2011.05.009.
[70] B.D. Manning, A. Toker, AKT/PKB signaling: navigating the network, Cell 169 (3) (2017) 381–405, http://dx.doi.org/10.1016/j.cell.2017.04.001.
[71] I.M. McGonnell, A.E. Grigoriadis, E.W.F. Lam, J.S. Price, A. Sunters, A specific role for phosphoinositide 3-kinase and AKT in osteoblasts? Front. Endocrinol. 3 (2012), http://dx.doi.org/10.3389/fendo.2012.00088.
[72] J. Liang, J. Zubovitz, T. Petrocelli, R. Kotchetkov, M.K. Connor, K. Han, et al., PKB/Akt phosphorylates p27, impairs nuclear import of p27 and opposes p27-mediated G1 arrest, Nat. Med. 8 (10) (2002) 1153, http://dx.doi.org/10.1038/nm761.
[73] A.J. Brown, E. Slatopolsky, Vitamin D analogs: therapeutic applications and mechanisms for selectivity, Mol. Asp. Med. 29 (6) (2008) 433–452, http://dx.doi.org/10.1016/j.mam.2008.04.001.
[74] G.L. Gravina, A. Mancini, C. Mattei, F. Vitale, F. Marampon, A. Colapietro, et al., Enhancement of radiosensitivity by the novel anticancer quinolone derivative vosaroxin in preclinical glioblastoma models, Oncotarget 8 (18) (2017) 29865–29886, http://dx.doi.org/10.18632/oncotarget.16168.
[75] R. Milani, E. Brognara, E. Fabbri, A. Finotti, M. Borgatti, I. Lampronti, et al., Corilagin induces high levels of apoptosis in the temozolomide-resistant T98G glioma cell line, Oncol. Res. Feat. Preclin. Clin. Cancer Ther. (2017), http://dx.doi.org/10.3727/096504017X14928634401187 [Epub ahead of print].
[76] S.Y. Lee, Temozolomide resistance in glioblastoma multiforme, Genes Dis. 3 (3) (2016) 198–210, http://dx.doi.org/10.1016/j.gendis.2016.04.007.
[77] I. Paw, R.C. Carpenter, K. Watabe, W. Debinski, H.W. Lo, Mechanisms regulating glioma invasion, Cancer Lett. 362 (1) (2015) 1–7, http://dx.doi.org/10.1016/j.canlet.2015.03.015.
[78] E. Garcion, N. Wion-Barbot, C.N. Montero-Menei, F. Berger, D. Wion, New clues about vitamin D functions in the nervous system, Trends Endocrinol. Metab. 13 (3) (2002) 100–105, http://dx.doi.org/10.1016/S1043-2760(01)00547-1.
[79] J. Moreno, A.V. Krishnan, D. Feldman, Molecular mechanisms mediating the antiproliferative effects of Vitamin D in prostate cancer, J. Steroid Biochem. Mol. Biol. 97 (1) (2005) 31–36, http://dx.doi.org/10.1016/j.jsbmb.2005.06.012.